Adıyaman University
Journal of Engineering Sciences
Adyü J Eng Sci 2026;13:e260106
Adıyaman Üniversitesi
Mühendislik Bilimleri Dergisi
Adyü Müh Bil Derg 2026;13:e260106
https://doi.org/10.54365/adyumbd.1842096

Research Article / Araştırma Makalesi

# Thermodynamic Analysis of an Integrated Organic Rankine Cycle (ORC) and Vapor Compression Cycle (VCC) with Internal Heat Exchangers using Next-Generation Working Fluids

## Yeni Nesil Çalışma Akışkanları Kullanılarak Dahili Isı Değiştiricili Entegre Organik Rankine Çevrimi (ORÇ) ve Buhar Sıkıştırma Çevriminin (BSÇ) Termodinamik Analizi

**Cenker Aktemur**[1] *

[1]Sivas University of Science and Technology, Faculty of Engineering and Natural Sciences, Mechanical Engineering Department, 58000, Sivas, Türkiye

**Öz**

Bu çalışmada, düşük küresel ısınma potansiyeline sahip çalışma akışkanları kullanılarak birleştirilmiş Organik Rankine Çevrimi–Buhar Sıkıştırmalı Soğutma Çevrimi (ORÇ–BSSÇ) sisteminin termodinamik analizi gerçekleştirilmiştir. ORÇ türbin güç çıktısı 1.795–1.962 kW aralığında değişmekte olup, çevrimin ısıl verimi 0.1008–0.1093 ve ekserji verimi 0.4347–0.4716 aralığındadır; her iki gösterge için yaklaşık %8.5'lik bir iyileşme elde edilmiştir. Soğutma sisteminde ise BSSÇ STK değeri 4.95'ten 5.303'e yükselirken, ekserji verimi 0.2622'den 0.2809'a çıkarak yaklaşık %7.1'lik bir artış göstermektedir. Toplam sistem açısından bakıldığında, genel STK 0.4989'dan 0.5799'a yükselmiş ve toplam ekserji verimi 0.1140'tan 0.1325'e çıkarak %16.2'lik bir iyileşme sağlamıştır. Parametrik analiz sonuçları, türbin giriş sıcaklığının artmasının hem STK hem de ekserji verimini artırdığını; buna karşılık kondenser sıcaklığındaki artışların performansı düşürdüğünü göstermektedir. İncelenen tüm çalışma akışkanı çiftleri arasında R1233zd(E)/R1336mzz(Z) çifti en yüksek termodinamik performansı sergilemiştir.

***Anahtar Kelimeler:*** *Organik Rankine Çevrimi, Buhar Sıkıştırmalı Çevrim, Soğutma Tesir Katsayısı, Ekserji Verimi, Küresel Isınma Potansiyeli*

**Abstract**

In this research, a thermodynamic analysis of a combined organic rankine cycle-vapor compression cycle (ORC-VCC) with low global warming potential working fluids is carried out. The ORC turbine power output varies between 1.795-1.962 kW, with thermal efficiency and exergy efficiency ranging between 0.1008-0.1093 and 0.4347-0.4716, respectively, showing a 8.5% relative improvement. In the refrigeration system, the VCC COP increases from 4.95 to 5.303, with a relative improvement in exergy efficiency of 7.1% from 0.2622 to 0.2809. The overall system COP increases from 0.4989 to 0.5799 with a 16.2% relative improvement in overall total exergy efficiency of 0.1140 to 0.1325. Parametric results show that higher turbine inlet temperatures improve both COP and exergy efficiency, while increased condenser temperatures reduce them. Amongst different fluid pairs investigated, R1233zd(e)/ R1336mzz(Z) shows best thermodynamic performance.

***Keywords:*** *Organic Rankine Cycle, Vapor Compression Cycle, Coefficient of Performance, Exergy Efficiency, Global Warming Potential*

* Corresponding e-mail (Sorumlu yazar e-posta): cenker.aktemur@sivas.edu.tr
**Received (Geliş Tarihi):**14.12.2025, **Accepted (Kabul Tarihi):** 28.01.2026

## 1. Introduction

The coupling of organic Rankine cycle (ORC) technology with vapor compression cycle (VCC) technology is a major breakthrough in energy conversion sciences and refrigeration engineering. The ORC is known for its potential to harness low-grade waste energies, thus providing useful work from waste energy sources [1-3]. The VCC, on the other hand, has been largely used in refrigeration systems, air-conditioning, and cold storage systems [4-6]. The ORC-VCC coupled system takes advantage of the strengths offered by the two different cycles, thus providing improved energy efficiencies and significant waste energy recovery [7]. This particular combined system is especially significant, as it integrates the turbine stages with the compressor stages on a shared shaft, thus minimizing, if not eliminating, the requirement for couplings, generators, and other mechanical/electrical equipment. This has potential implications with respect to reduced operating and maintenance costs because of optimized systems. Over the last decade, research has been largely invested in the evaluation of different configurations of ORC-VCC systems [8-10].

ORC-VCC systems have been extensively researched with a diverse set of focuses, including a modeling work on the thermodynamics [11], economic viability [12], and working fluid choice [13]. The root reason behind such research is the aim to optimize efficiency as well as improve waste heat conversion, especially whenapplicable on a small scale, which is highly cost-effective from a savings perspective as well as has a distinctively high potential to address planet-friendly goals [13,14]. Recent experiments have generated significant research on ORC-VCC systems. In reference [15], the authors specifically investigated the non-design performance efficiency of an ORC-VCC setup that used the low-global warming potential (GWP) refrigerants R1234ze(E). The experiment clearly revealed that with an increase in the condenser heat rejection temperatures from 30°C to 16.6°C, the system's COP varied from 0.558 to 0.682. Additionally, a rise in the driving heat source temperatures led to increased COP for ORC, but with a corresponding drop in the efficiency of the compressor. Another significant experimental validation [16] clearly identified that when ORC-VCC is considered on a 264 kWth setup, with a condenser heat rejection temperature at 30°C, the resulting COP of 0.56 is obtained when the low-GWP working fluid R1234ze(E), a next-generation refrigerant, is used. The authors also identified that the system is significantly dependent on external factors such as condenser temperatures, evaporator temperatures, etc. The similar findings are observed in reference [17], where the authors specifically experimented with the thermo-mechanical cooling setup with ultra-low-temperature waste heat application. The authors primarily identified that with a rise in heat source temperatures, efficiency improved, although not optimally but with specific conditions. The authors specifically identified that because of the adoption of optimum working conditions, the efficiency of ORC-VCC setup improves significantly. An essential element that hampers ORC-VCC setup efficiency is the choice of refrigerants. Although the choice is characteristic, it has high GWP, resulting in a high potential threat to the environment; therefore, significant research has been initiated on adapting a low-GWP environment, which is eco-friendly to a large extent, thereby meeting distinct environment-friendly goals [18].

Recently, considerable theoretical research has been carried out on the ORC-VCC system. Various works on the selection of the working fluid, which is a key part in the overall design of the ORC-VCC system, have been done. Gonzalez et al. [23] carried out a comparison on the COP of the ORC-VCC system with various working fluids. Based on the analysis, the study found that the best working fluid with the highest COP is the R1233zd(E) + n-Pentane fluid pair. On the other hand, Bouneful et al. [24] found that the thermodynamic performance of the R600 fluid is the best among the fluids analyzed. From the energy and exergy analysis carried out on the ORC-VCC system, Ngangúe et al. [25] found that the R717 fluid is an excellent fluid that can be used in the overall process. Based on the thermo-economic analysis carried out on the overall process, Zhar et al. [26] found that the R123 fluid is the best fluid that can be used in the overall process. Based on the analysis carried out on the overall process, Xia et al. [27] found that hydrocarbon fluids are the best fluids that can be used in the overall process. From the above analysis, the divergence among the works carried out on the overall process indicates that the best fluid that can be

used in the overall process depends on the analysis carried out on the overall process. This divergence among the works carried out on the overall process can be explained by the fact that the analysis carried out on the overall process is limited to a few fluids. Furthermore, the overall process can be carried out with pure fluids.

Compared to pure working fluids, the irreversibilities in the phase change heat transfer processes of zeotropic mixtures can be minimized by the characteristics of the temperature slip. Zheng et al. [28] indicated that the binary mixtures achieve a greater thermal efficiency compared to the pure fluids in the ORC-VCC arrangement. Moreover, the study by Ashwni et al. [29] revealed that there is an optimum mass fraction for the mixtures, as the ORC-VCC system reaches the maximum COP when the mass fraction is 0.6 for the Hexane/R245fa blend. Moreover, some research has performed parametric analysis of the ORC-VCC system. Karellas and Braimakis [30] stated that increasing the evaporation temperature of the VCC system would improve the energy efficiency, exergy efficiency, COP, as well as the power generated, while the opposite would happen when increasing the condensation temperature. Bu et al. [22] proposed that there would be an optimal temperature at which the efficiency of the ORC-VCC system would be maximized in order to produce the maximum efficiency in the system as a whole. Furthermore, increasing the COP of the ORC-VCC system would result from increasing the system's heat source temperature as well as its evaporation temperature, while decreasing the system's condensation temperature would result in a decrease in its COP, according to Saleh's research, which was followed in this study as well as in Ref. [32] in which increasing the system's condensation pressure would result in a decrease in its thermal efficiency as well as its exergy efficiency. Moreover, Ref. [23] stated that increasing the COP of the ORC-VCC system would result from decreasing its condensation temperature, while Nasir and Kim [27] stated that increasing the outdoor temperature from 30°C to 40°C would result in increasing the total COP of the system from 0.172 to 0.217, while Bao et al. [33] stated that the efficiency of the dual-fluid ORC-VCC system would be higher compared to that of the single-fluid system, while Alshammari et al. [21] proposed a novel single-rotor expander-compressor system in order to improve the efficiency of the ORC-VCC system, which reached a maximum efficiency of 56% as a result of its ability to produce a maximum cooling capacity of 5.38 kW.

A comprehensive review of the relevant literature revealed that studies focusing on the exploration and assessment of the next generation of low-GWP working media for the combined system of integrated ORCs and VCCs are still scarce. In this context, this study aims to address this knowledge gap by proposing and thermodynamically investigating a system of combined ORCs and VCCs and exploring the influence of different pairs of next-generation working media. The energy and exergy analysis of the system will be conducted for a series of scenarios regarding different working fluid pairs. The energy and exergy assessment of the ORCs and VCCs will include the calculation of the power output, thermal efficiency, COP, and exergy efficiency. The overall energy and exergy assessment will include the calculation of the COP and exergy efficiency for the overall system. The thermodynamic model will include mass balance equations, energy balance equations, and exergy balance equations for each component of the system. The proposed system will include the calculation of the relevant thermophysical properties of the working fluid. The proposed system will serve as a novel and original method for exploring and assessing the sensitivity of the overall system.

## 2. Material and Method

The performance of the VCC is assessed for a fixed cooling capacity of 10 kW, from which the refrigerant mass flow rate, power consumption, and COP are calculated. In ORC components, the power generated by the turbine is considered to power the VCC compressor directly, while the net power generated is calculated by subtracting the power consumed by the pump from that generated by the turbine [13]. The thermal efficiency of ORC is calculated based on the net power generated per unit of heat input to the evaporator. The exergy analysis of both systems is carried out with a reference ambient temperature of 298.15 K. The exergy efficiency of the ORC is calculated on the basis of exergy of the heat input, whereas

that of the VCC is calculated on the basis of the exergy of the cooling effect. The exergy efficiency of the entire process is obtained by integrating the exergy efficiency of the ORC and VCC, thus taking a complete account of the irreversibilities existing within the combined process.

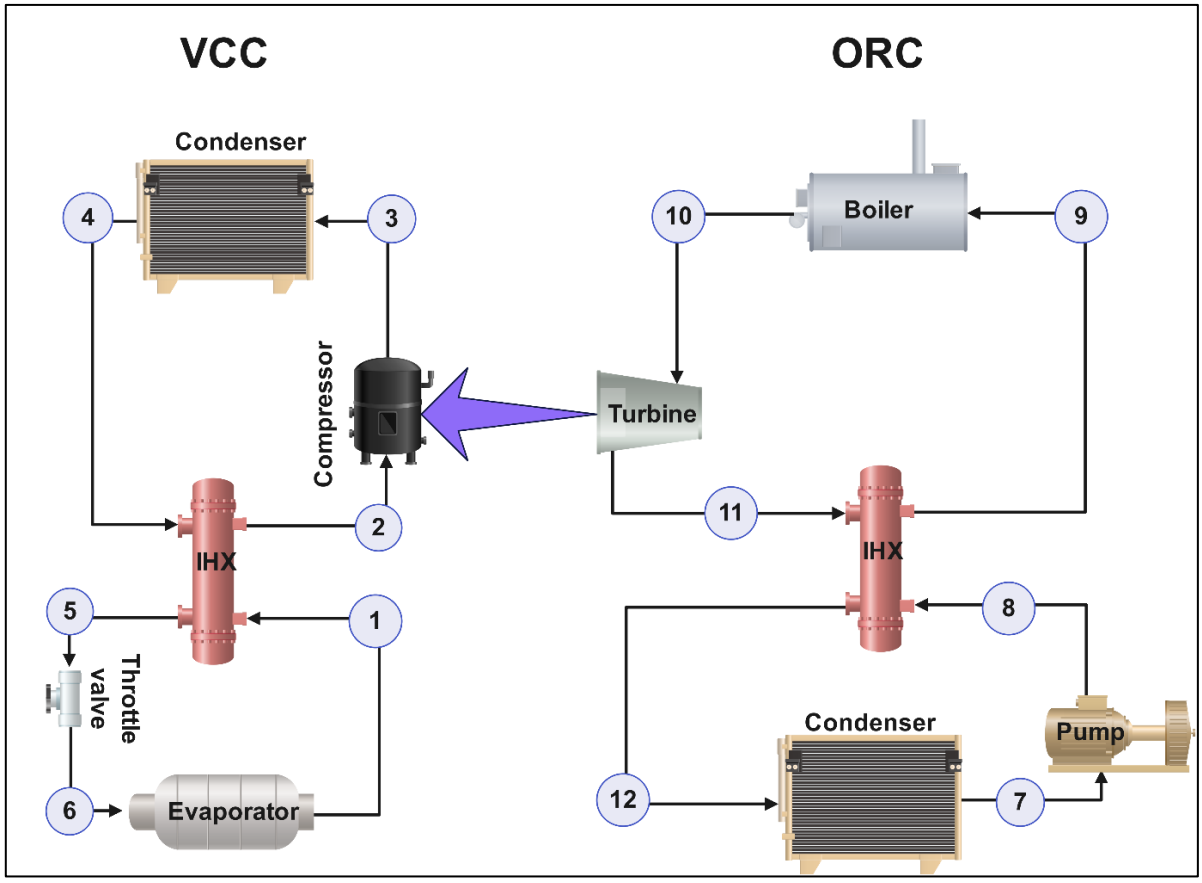


**Figure 1.** Schematic presentation of an integrated ORC-VCC system

In the present study, the entire system is evaluated under steady-state and steady-flow operating conditions to ensure that all thermodynamic properties and mass flow rates remained constant over time. Frictional pressure drops in piping and heat exchangers, as well as external heat losses to the environment, are assumed to be negligible, allowing the analysis to focus solely on the dominant thermodynamic interactions within the ORC and VCC. Variations in kinetic and potential energies of the working fluids are also neglected, given their insignificant contribution compared to the thermal and mechanical energy terms. Furthermore, it was assumed that the mechanical power produced by the ORC expander is entirely transferred to and consumed by the VCC compressor, ensuring a direct mechanical coupling between the two subsystems. Finally, the throttling process in the VCC expansion valve is modeled as an isenthalpic process, consistent with standard VCC assumptions and supported by negligible kinetic energy effects at the inlet and outlet of the valve [13,18,19].

The numerical analysis of the thermodynamic performance for the conceptual integrated system was carried out using the Engineering Equation Solver (EES) software platform. EES solutions for thermodynamic properties, state points, and numerical performance factors were achieved through the development of an extensive set of EES equations. These equations were developed with continuity with accepted models for numerical representation of thermodynamic properties as documented in the literature [9-11, 13, 15], thereby ensuring consistency of numerical solutions. These EES models include mass balances, energy balances, expressions for the efficiency of system components, as well as expressions for the thermophysical properties of the fluids of choice. In order to improve clarity for independent verification of this numerical analysis study, the detailed EES equations organized for this numerical solution study are systematically documented in Tables 1-5.

The ORC-VCC system was modeled based on a steady-state solution with a component-level thermodynamic approach. The ORC-VCC were initially developed separately before combining them with a turbine-compressor power balance technique [13,19]. In modeling the VCC, R1234yf, R1234ze(E), R1224yd(Z) and R1233zd(E) were used, but R1233zd(E), R1224yd(Z), R1234ze(Z) and R1336mzz(Z) were considered for the ORC. Under the fixed operating conditions, the temperature of the VCC evaporator outlet was set to 5°C, but the condenser outlet temperature was set to 40°C [19]. In addition, for the ORC, the inlet temperature of the turbine component was set to 100°C, but the condenser outlet temperature was set to 40°C [19]. The isentropic efficiencies for the compressor and turbine were assumed to be 0.75 [19], but the efficiency for the pump is 0.80 [13,19]. An internal heat exchanger (IHX) is added to both cycles, with an effectiveness of 0.70 [20]. The properties, such as enthalpy and entropy, are calculated from temperature-pressure and temperature-quality curves.

**Table 1.** Input parameters and values

| Variable | Value | Description |
|---|---|---|
| T0 | 298.15 | Ambient temperature [°C] |
| T_source | T10 + 273.15 + 15 | Source temperature [°C] |
| T_space | T1+273.15+5 | Space temperature [°C] |
| T1 | -10 - 10 | Evaporator outlet temperature (VCC) [°C] |
| T4 | 35 - 50 | Condenser outlet temperature (VCC) [°C] |
| T7 | 35 - 50 | Condenser outlet temperature (ORC) [°C] |
| T10 | 80 - 120 | Evaporator outlet / turbine inlet temperature (ORC) [°C] |
| x1 | 1 | Saturated vapor at VCC evaporator outlet |
| x4 | 0 | Saturated liquid at VCC condenser outlet |
| x7 | 0 | Saturated liquid at ORC condenser outlet |
| x10 | 1 | Saturated vapor at ORC turbine inlet |
| eta_pump | 0.80 | Isentropic efficiency of pump |
| eta_turb | 0.75 | Isentropic efficiency of turbin |
| eta_comp | 0.75 | Isentropic efficiency of compressor |
| ε | 0.70 | Effectiveness of internal heat exchanger |

**Table 2.** Pressure relations for the integrated VCC–ORC system

| Cycle | State | Pressure Relation | Physical Meaning |
|---|---|---|---|
| VCC | P1 | P1 = pressure(R*, T=T1, x=x1) | Evaporator pressure |
| | P2 | P2 = P1 | IHX cold-side pressure (no pressure drop) |
| | P6 | P6 = P1 | Pressure after expansion valve |
| | P4 | P4 = pressure(R*, T=T4, x=x4) | Condenser pressure |
| | P5 | P5 = P4 | IHX hot-side exit pressure |
| | P3 | P3 = P4 | Compressor discharge pressure |
| ORC | P7 | P7 = pressure(RR*, T=T7, x=x7) | ORC condenser pressure |
| | P12 | P12 = P7 | Recuperator hot-side exit pressure |
| | P11 | P11 = P7 | Turbine outlet pressure |
| | P10 | P10 = pressure(RR*, T=T10, x=x10) | ORC evaporator pressure |
| | P9 | P9 = P10 | Recuperator cold-side pressure |
| | P8 | P8 = P10 | Pump discharge pressure |

*R and RR mean the fluids used in VCC and ORC, respectively.

**Table 3.** VCC state equations, mass balance, and performance relations

| Category | Variable | Equation | Description |
|---|---|---|---|
| State 1 | h1 | h1 = enthalpy(R, T=T1, x=x1) | Evaporator outlet enthalpy |
| | s1 | s1 = entropy(R, T=T1, x=x1) | Evaporator outlet entropy |
| State 2 | T2 | T2 = T1 + ε ·(T4 − T1) | IHX cold exit temperature |
| | h2 | h2 = enthalpy(R, T=T2, P=P2) | Compressor inlet enthalpy |
| | s2 | s2 = entropy(R, T=T2, P=P2) | Compressor inlet entropy |
| State 3 | s3s | s3s = s2 | Isentropic reference |
| | h3s | h3s = enthalpy(R, P=P3, s=s3s) | Isentropic outlet enthalpy |
| | h3 | h3 = h2 + (h3s − h2)/eta_komp | Real compressor outlet enthalpy |
| | T3 | T3 = temperature(R, P=P3, h=h3) | Compressor outlet temperature |
| | s3 | s3 = entropy(R, P=P3, h=h3) | Compressor outlet entropy |
| State 4 | h4 | h4 = enthalpy(R, T=T4, x=x4) | Condenser outlet enthalpy |
| | s4 | s4 = entropy(R, T=T4, x=x4) | Condenser outlet entropy |
| State 5 | h5 | h5 = h4 − (h2 − h1) | IHX hot-side energy balance |
| | T5 | T5 = temperature(R, P=P5, h=h5) | Valve inlet temperature |
| | s5 | s5 = entropy(R, P=P5, h=h5) | Valve inlet entropy |
| State 6 | h6 | h6 = h5 | Isenthalpic expansion |
| | T6 | T6 = temperature(R, P=P6, h=h6) | Expansion valve outlet temperature |
| | s6 | s6 = entropy(R, P=P6, h=h6) | Expansion valve outlet entropy |
| Mass balance | ṁ1–ṁ6 | ṁ1 = ṁ2 = ṁ3 = ṁ4 = ṁ5 = ṁ6 | Steady-state continuity |
| Performance | Q̇_evap | Q̇_evap = ṁ1 ·(h1 − h6) | Cooling capacity |
| | Q̇_cond | Q̇_cond = ṁ1 ·(h3 − h4) | Condenser heat rejection |
| | Q̇_comp | Ẇ_comp = ṁ1 ·(h3 − h2) | Compressor power |
| | COP | COP = Q̇_evap / Ẇ_comp | VCC coefficient of performance |

**Table 4.** ORC state equations, mass balance, and performance relations

| Category | Variable | Equation | Description |
|---|---|---|---|
| State 7 | h7 | h7 = enthalpy(RR, T=T7, x=x7) | Condenser outlet enthalpy |
| | s7 | s7 = entropy(RR, T=T7, x=x7) | Condenser outlet entropy |
| State 8 | s8s | s8s = s7 | Isentropic pump reference |
| | h8s | h8s = enthalpy(RR, P=P8, s=s8s) | Isentropic pump outlet |
| | h8 | h8 = h7 + (h8s − h7)/eta_pump | Real pump outlet enthalpy |
| | T8 | T8 = temperature(RR, P=P8, h=h8) | Pump outlet temperature |
| | s8 | s8 = entropy(RR, P=P8, h=h8) | Pump outlet entropy |
| State 9 | T9 | T9 = T8 + ε ·(T11 − T8) | Recuperator cold exit temperature |
| | h9 | h9 = enthalpy(RR, T=T9, P=P9) | Recuperator cold exit enthalpy |
| | s9 | s9 = entropy(RR, T=T9, P=P9) | Recuperator cold exit entropy |
| State 10 | h10 | h10 = enthalpy(RR, T=T10, x=x10) | Turbine inlet enthalpy |
| | s10 | s10 = entropy(RR, T=T10, x=x10) | Turbine inlet entropy |
| State 11 | s11s | s11s = s10 | Isentropic turbine reference |
| | h11s | h11s = enthalpy(RR, P=P11, s=s11s) | Isentropic turbine outlet |
| | h11 | h11 = h10 − eta_turb ·(h10 − h11s) | Real turbine outlet enthalpy |
| | T11 | T11 = temperature(RR, P=P11, h=h11) | Turbine outlet temperature |
| | s11 | s11 = entropy(RR, P=P11, h=h11) | Turbine outlet entropy |
| State 12 | h12 | h12 = h11 − (h9 − h8) | Recuperator energy balance |
| | T12 | T12 = temperature(RR, P=P12, h=h12) | Recuperator hot exit temperature |
| | s12 | s12 = entropy(RR, P=P12, h=h12) | Recuperator hot exit entropy |
| Mass balance | ṁ7–ṁ12 | ṁ7 = ṁ8 = ṁ9 = ṁ10 = ṁ11 = ṁ12 | Steady-state continuity |
| Performance | Q̇_in | Q̇_in = ṁ7 ·(h10 − h9) | ORC heat input |
| | Q̇_out | Q̇_out = ṁ7 ·(h12 − h7) | ORC heat rejection |
| | Ẇ_turb | Ẇ_turb = ṁ7 ·(h10 − h11) | Turbine power |
| | Ẇ_pump | Ẇ_pump = ṁ7 ·(h8 − h7) | Pump power |
| | Ẇ_net | Ẇ_net = Ẇ_turb − Ẇ_pump | Net ORC power |
| | eta_ORC | eta_ORC = Ẇ_net / Q̇_in | ORC thermal efficiency |
| | COP_all | COP_all = eta_ORC ·COP | Overall system COP |

**Table 5.** Exergy Analysis Equations

| Parameter | Equation |
|---|---|
| ORC heat exergy | Ex_Q̇_in_ORC = Q̇_in ·(1 − T0 / T_source) |
| ORC exergy efficiency | eta_ex_ORC = Ẇ_net / Ex_Q̇_in_ORC |
| Space temperature | T_space = T1 + 273.15 + 5 |
| Cooling exergy | Ex_cooling_VCC = Q̇_evap ·(T0 / T_space − 1) |
| VCC exergy efficiency | eta_ex_VCC = Ex_cooling_VCC / Ẇ_comp |
| Overall system exergy efficiency | eta_sys = eta_ex_VCC ·eta_ex_ORC |

## 3. Results and Discussion

### 3.1 Model validation

For the validation of the developed ORC–VCC model, the same operating conditions were used as for the experimental ORC–VCC system implemented by Grauberger et al. [16]. In the course of the validation, the temperature of the waste heat source used for the operation of the ORC–VCC system (91 °C), the temperature range of the condenser's inlet and outlet (30–36 °C), the range of the evaporator's operation (12–7 °C), the used refrigerant R1234ze(E), the isentropic efficiencies of the turbine and the compressor, the temperature difference of the pinch point, the level of sub-cooling/super-heating, and the pressure losses were used under the same conditions as described in the above-mentioned study. The validated results have shown a deviation range of 7-8% from the experimental data reported by Grauberger et al. [16]. This confirms that the developed model can be relied upon to simulate the thermodynamic behavior under the same operating conditions.

**Table 6.** Model validation against the experimental ORC–VCC data reported by Grauberger et al. (2022).

| Parameter | Grauberger et al. [16] | This study | Deviation |
|---|---|---|---|
| Condenser heat load of ORC | 435.7 kW | 468 kW | +7.4% |
| Condenser heat load of VCC | 291.8 kW | 315 kW | +7.9% |
| Thermal efficiency of ORC | 7.71% | 8.28% | +7.4% |
| COP of VCC | 5.23 | 5.62 | +7.5% |

### 3.2 Fixed Operating Condition Analysis

In this study, the ORC–VCC organic fluid pairs examined are coded from FP-1 to FP-16 to improve the presentation of results and the readability of Figures 2-8. Interpretations and comparisons of the fluid pairs are made using these codes, without repeating fluid names in the text. The same coding system is used in Figures 2-8, with each FP code representing a specific VCC–ORC fluid combination. The fluid pairs represented by the codes are FP-1 → R1234yf / R1233zd(E), FP-2 → R1234yf / R1224yd(Z), FP-3 → R1234yf / R1234ze(Z), FP-4 → R1234yf / R1336mzz(Z), FP-5 → R1234ze(E) / R1233zd(E), FP-6 → R1234ze(E) / R1224yd(Z), FP-7 → R1234ze(E) / R1234ze(Z), FP-8 → R1234ze(E) / R1336mzz(Z), FP-9 → R1224yd(Z) / R1233zd(E), FP-10 → R1224yd(Z) / R1224yd(Z), FP-11 → R1224yd(Z) / R1234ze(Z), FP-12 → R1224yd(Z) / R1336mzz(Z), FP-13 → R1233zd(E) / R1233zd(E), FP-14 → R1233zd(E) / R1224yd(Z), FP-15 → R1233zd(E) / R1234ze(Z) and FP-16 → R1233zd(E) / R1336mzz(Z).

The result of the comparative performance evaluation of the combined ORC-VCC system clearly indicates a strong dependence on the working fluid pair (FP-1 to FP-16). This section analyzes the performance of the combined ORC-VCC system on the basis of seven major performance criteria through Figure 2 to 8. In this regard, the ORC system is assessed on the basis of turbin power output and thermal efficiency as well as exergy efficiency, while the assessment of the VCC is carried out in terms of the Coefficient of Performance (COP), in addition to exergy efficiency. The performance analysis of the combined ORC-VCC system is carried out on the basis of the overall COP and overall exergy efficiency.

The alteration of turbin power output with combination of working pair is shown in Figure 2. Modest fluctuations of the turbine power output are noticed for the combined ORC-VCC system using the sixteen working fluid pairs, namely FP-1 through FP-16, with power outputs varying between 1.795 kW and 1.962 kW. The maximum power is found for FP-4 with a power output of 1.962 kW, followed by FP-1 with 1.945 kW and FP-2 with 1.930 kW. This implies that the thermophysical properties of the working fluids in FP-4 make it more feasible for expansion in the ORC turbine, thereby ensuring better power recovery. Contrarily, the lowest power outputs of the turbines occur for FP-15 with a value of 1.795 kW and for FP-11 with a value of 1.799 kW, indicating a drop of about 8.5% from the maximum power output. Most of the fluid pairs lie between the levels of 1.80 kW and 1.90 kW, which implies that despite the effect of the fluid on turbine power output, there is a certain limit beyond which the power output of the turbine cannot fall.

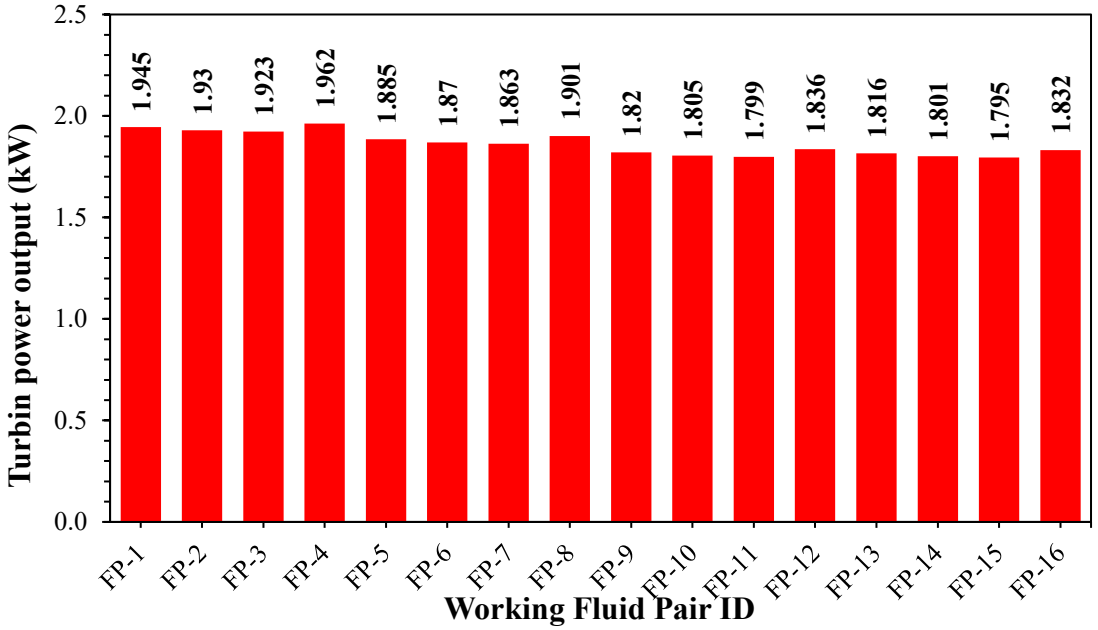


**Figure 2.** The alteration of turbin power output with combination of working pair

The alteration of thermal efficiency of ORC with combination of working pair is shown in Figure 3. A small but regular variation of the thermal efficiency of the ORC is observed for the sixteen working fluid pairings (FP-1 to FP-16), ranging from 0.1008 to 0.1093. While the peak thermal efficiency of ORC of 0.1093 is established for FP-4, FP-8, FP-12, and FP-16, there is a regular pattern related to these fluid pairings. On the other hand, the lowest thermal efficiency of 0.1008 is established for FP-3, FP-7, FP-11, and FP-15, with an efficiency loss of about 7.8% compared to the best cases. The intermediate values of efficiency for 0.1064 (FP-1, FP-5, FP-9, FP-13) and 0.1054 (FP-2, FP-6, FP-10, FP-14) provide further evidence of the presence of two clusters, pointing to the significant effect of the thermophysical matching of the respective working fluid pairs on the thermal efficiency of the ORC, rather than random factors. The range is limited by 0.0085 in absolute values. Despite the small differences in number, these differences are no longer negligible for integrated ORC-VCC systems, since even small improvements in the efficiency of the ORC process are always beneficial to the total power output of the system. It is evident that the selection of appropriate fluids is important for improving the thermal efficiency of the ORC process by almost 8%.

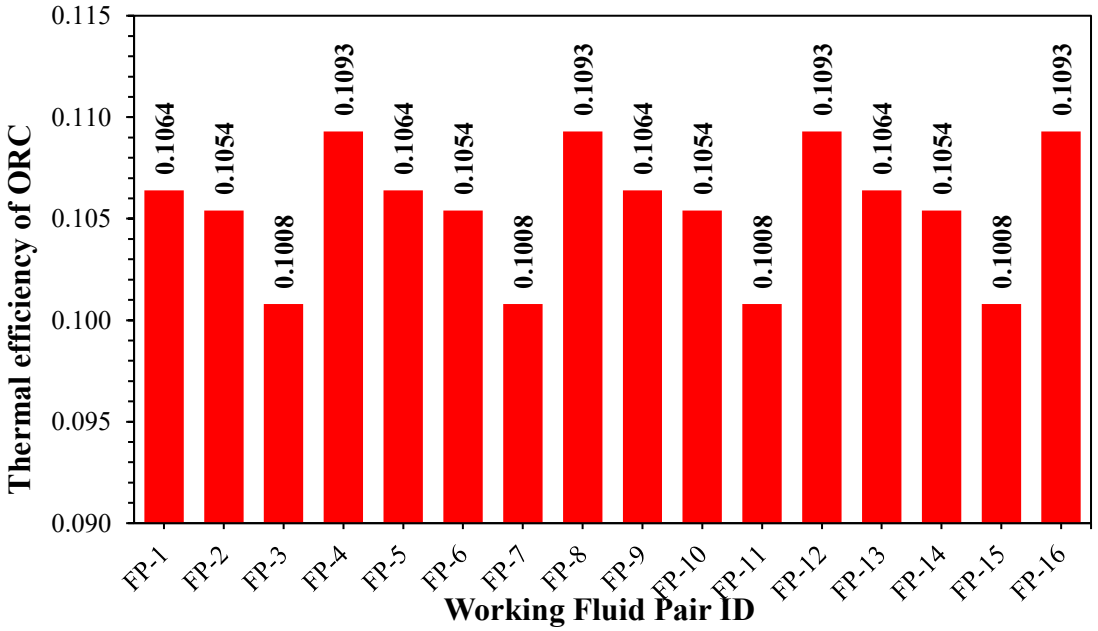


**Figure 3.** The alteration of thermal efficiency of ORC with combination of working pair

The alteration of COP of VCC with combination of working pair is shown in Figure 4. COP of the VCC varies in a stepwise incremental manner with the COP ranging between 4.95 and 5.303 for the sixteen working fluids. A low of 4.95 COP is found for FP-1 through FP-4, implying that these fluids work less effectively as refrigerants. A moderate improvement is achieved for FP-5 through FP-8, with a gradual increase in COP to 5.108, representing an improvement of about 3.2% over the lowest group. Further improvement is found for FP-9 through FP-12, with a COP of 5.291 in all of them, indicating that there is a 6.9% improvement over FP-1 through FP-4. The maximum COP of 5.303 is maintained for FP-13 through FP-16, indicating that there is an average improvement of 7.1% with respect to the lowest point. This gradual increase suggests that VCC strongly depends on the chosen working fluid pair, especially through its influence on compressor work and the refrigeration effect. While apparently small in each group, the limited dispersion of the data and the monotonic behavior of the COP for each group indicate that the VCC is functioning in a stable, predictable way while still reaping the rewards of optimized working fluid combinations. When taken in context with the performance data for the ORC, the high COP values for FP-13 through FP-16 are of great importance since they directly influence the enhanced COP_all of the combined ORC-VCC system.

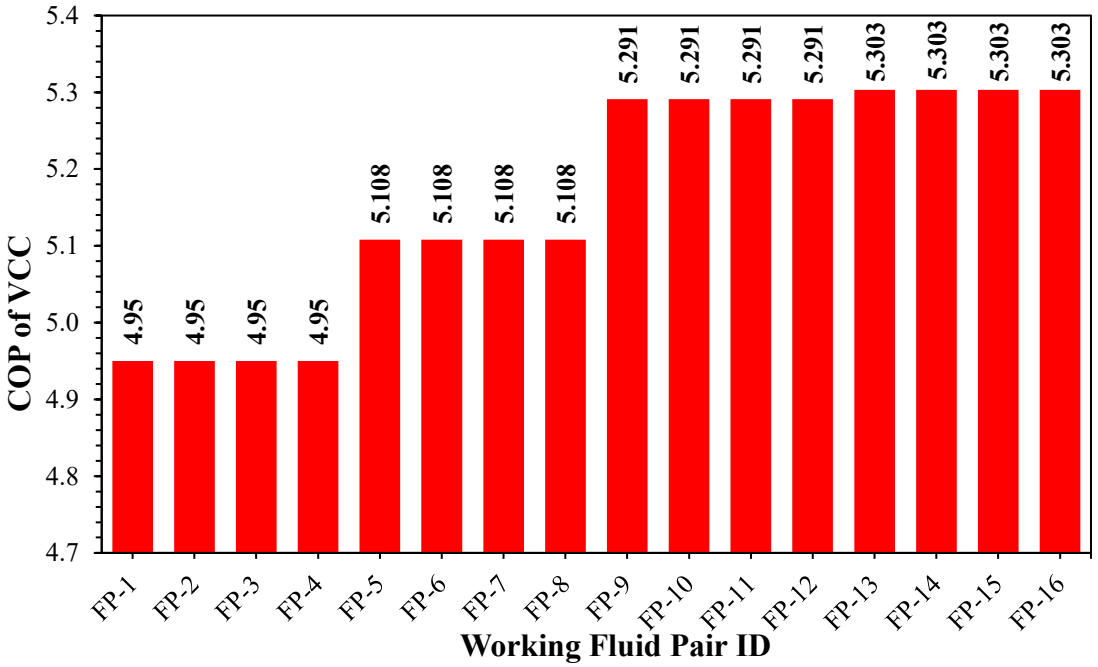


**Figure 4.** The alteration of COP of VCC with combination of working pair

The alteration of overall COP of combined system with combination of working pair is shown in Figure 5. Overall COP for the integrated ORC-VCC system varies significantly with the selected working fluid combination, which ranges from 0.4989 to 0.5799 for the FP-1 to FP-16 fluid pair. The lowest overall performance is found for FP-3 with COP_all = 0.4989, whereas the maximum COP_all of 0.5799 is achieved with FP-16. This is approximately an improvement of 16.2% for the lowest to the best-working fluid combination. There is a gradual enhancement of overall COP with the progress of the working fluid pairs, especially after FP-7. Relatively moderate values between 0.5269 and 0.5438 exist for FP-1 to FP-5, but a substantial escalation is seen for FP-8 to FP-10, where COP_all is well over 0.558. The significantly high values of overall COP of 0.5786 for FP-12 and overall COP of 0.5799 for FP-16.

The alteration of exergy efficiency of ORC with combination of working pair is shown Figure 6. The exergy efficiency of the ORC varies systematically among the sixteen working fluid pairs, with a minimum of 0.4347 and a maximum of 0.4716. It is noted that the lowest exergy efficiency of 0.4347 is for FP-3, FP-7, FP-11, and FP-15, whereas the maximum of 0.4716 is for FP-4, FP-8, FP-12, and FP-16. Moreover, the absolute difference between the lowest and the highest is 0.0369, signifying that the efficiency difference

is by approximately 8.5%. Apart from the mentioned extremes, there are two levels for intermediate efficiency: 0.4591 for FP-1, FP-5, FP-9, and FP-13; and 0.4544 for FP-2, FP-6, FP-10, and FP-14.

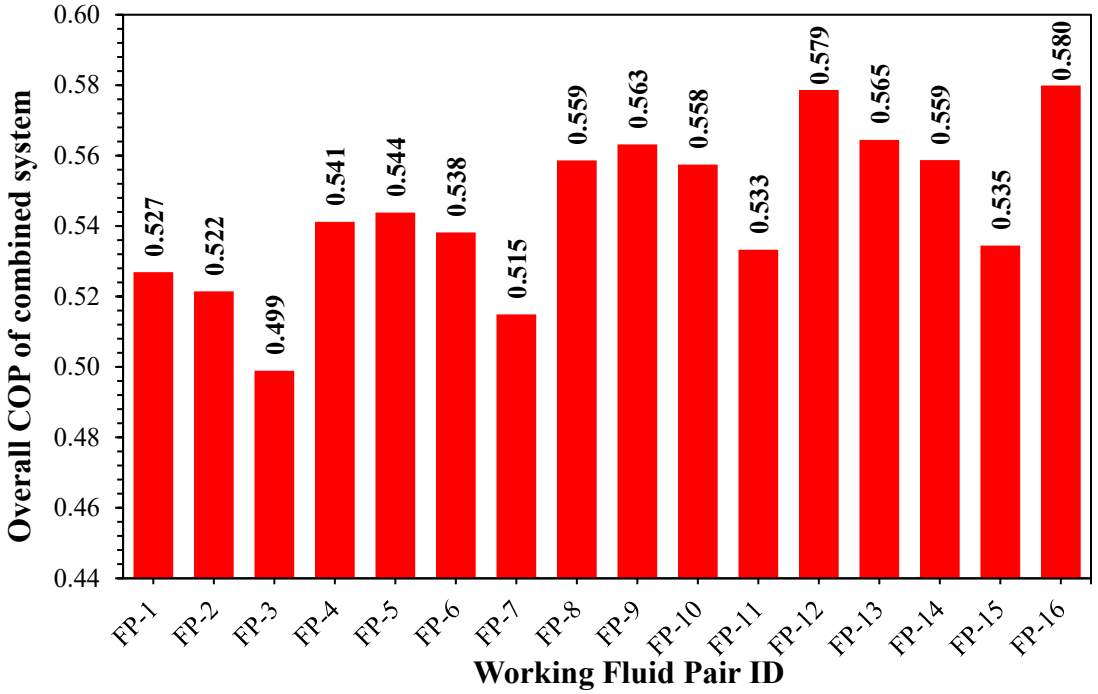


**Figure 5.** The alteration of overall COP of combined system with combination of working pair

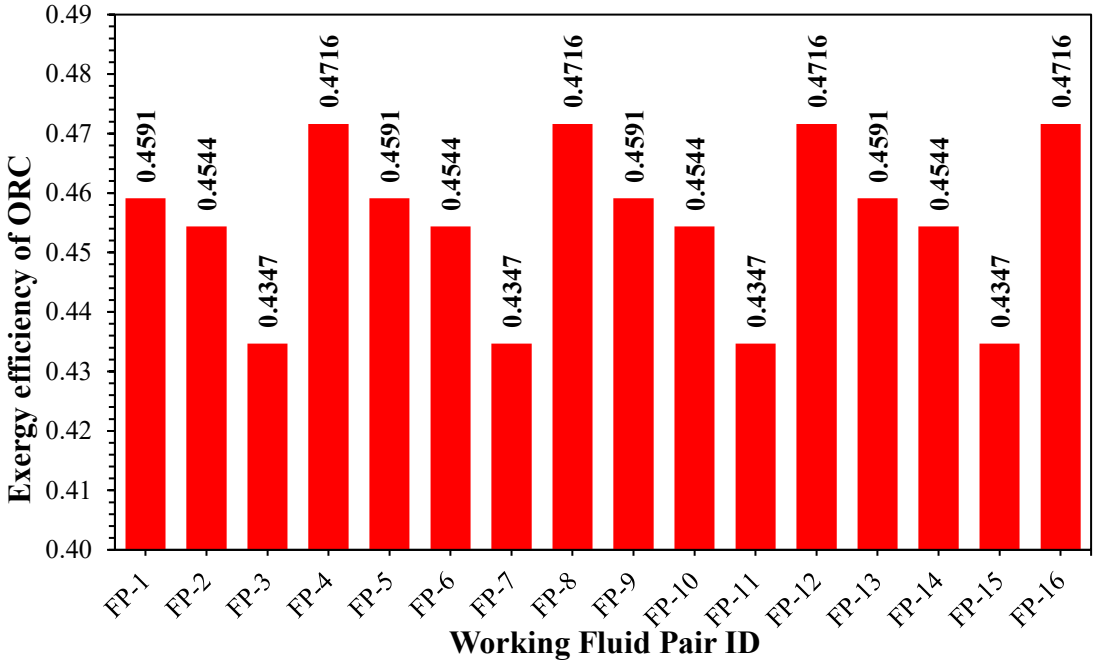


**Figure 6.** The alteration of exergy efficiency of ORC with combination of working pair

The alteration of exergy efficiency of VCC with combination of working pair is shown in Figure 7. The exergy efficiency of the VCC shows a progressive increase with the changing refrigerants, which varies from 0.2622 to 0.2809. The lowest efficiency (0.2622), signifying high irreversibilities in the compression process, is observed in systems with R1234yf (FP-1-FP-4). The use of R1234ze(E) improves exergy efficiency of VCC to 0.2706, while R1224yd(Z) improves it to 0.2803. The highest exergy efficiency of 0.2809 is obtained with R1233zd(E) (FP-13-FP-16), thus providing a total improvement of about 7%, which is a sign of low exergy destruction and improved compatibility of the VCC.

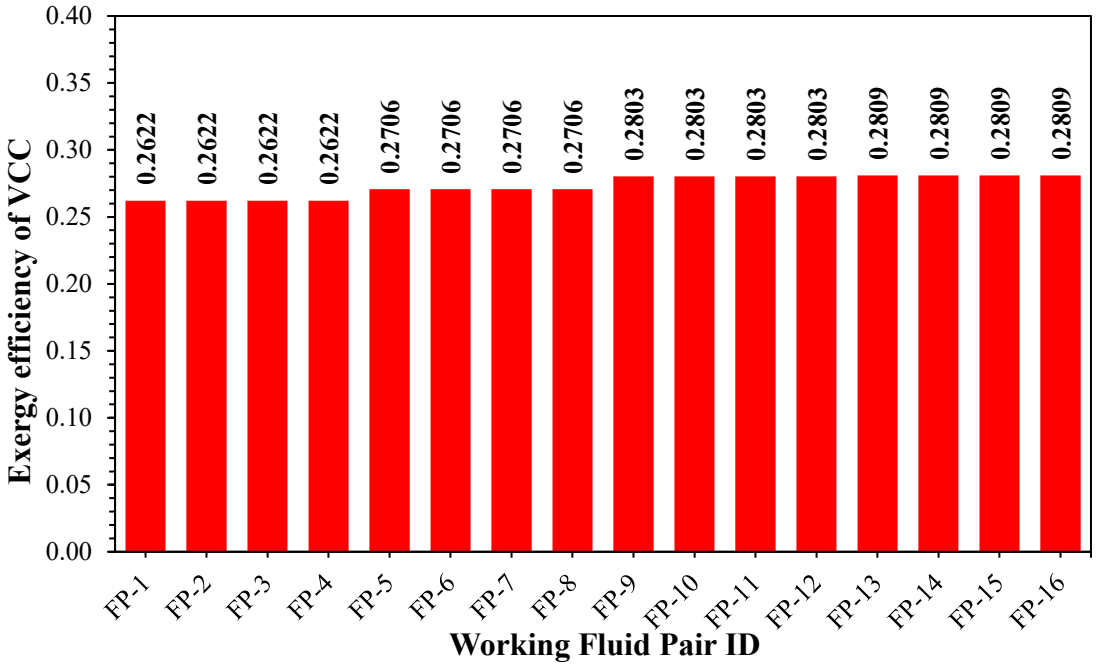


**Figure 7.** The alteration of exergy efficiency of VCC with combination of working pair

The alteration of exergy efficiency of combined system with combination of working pair is shown in Figure 8. The total exergy efficiency for the system, represented by the combined efficiency of the ORC and VCC, varies between 0.1140 and 0.1325 for the sixteen distinct work fluids. The lowest total efficiency of 0.1140 is for FP-3, whereas the maximum total efficiency of 0.1325 is for FP-16. This is accompanied by an absolute improvement of 0.0185, or a relative improvement of approximately 16.2%. Values of 0.1276 for FP-8, 0.1287 for FP-9, and 0.1322 for FP-12 represent an appreciable positive drift of the total exergy efficiency of the system with respect to the work fluid pair number. It is evident that higher values of total exergy efficiency correlate with instances having the absolute efficiency of both cycles numerically higher. Of all the cases explored, FP-12 and FP-16 exhibit distinctiveness in keeping their total exergy efficiency values consistently above 0.13, thereby signifying that these work fluids present better performance.

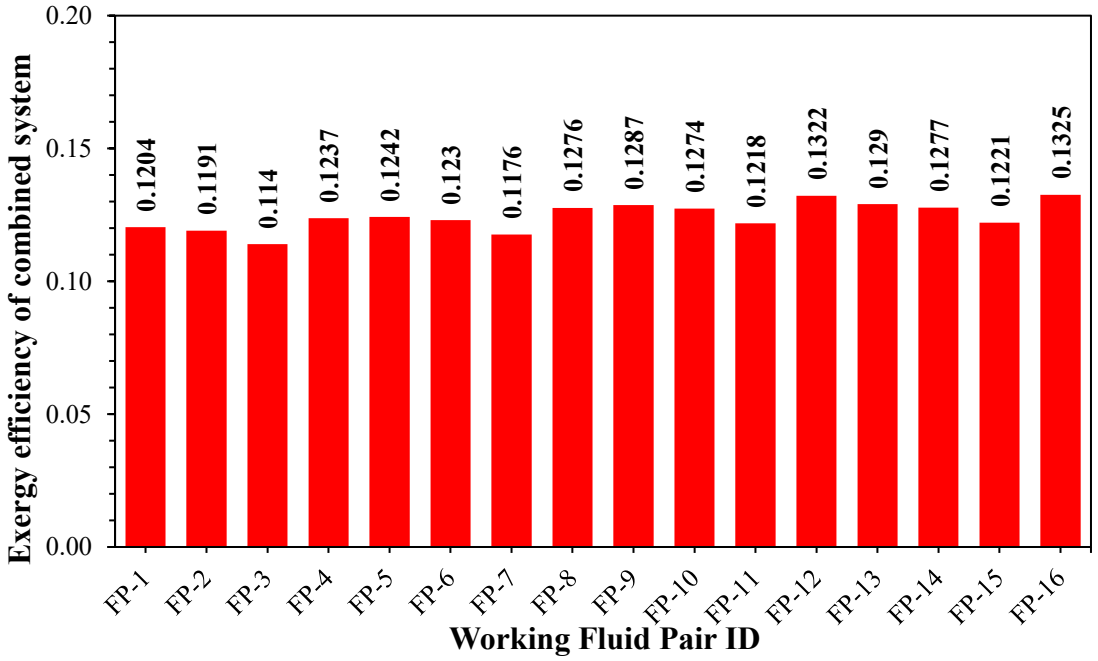


**Figure 8.** The alteration of exergy efficiency of combined system with combination of working pair

### 3.3 Parametric analysis

On the basis of the initial comparison of performance carried out at a fixed operating temperature, R1233zd(E) and R1336mzz(Z) have the maximum overall COP as well as overall exergy efficiency values compared to other working fluids. Thus, a parametric study of the combined ORC-VCC system was carried out only for R1233zd(E) and HFO-1336mzz(Z).

The variation of overall COP and exergy efficiency of ORC-VCC system with turbin inlet temperature is shown in Figure 9. With the increase in the turbine inlet temperature from 80 °C to 120 °C, there is a steady increase in the value of the overall COP and the overall exergy efficiency of the integrated ORC-VCC system. The value of the overall COP rises from 0.1173 to 0.1395, indicating a relative improvement of about 19%. This can be related to the fact that the expansion work output of the ORC turbine increases with a rise in the turbine inlet temperature, thereby reducing the work of compression of the VCC subsystem. Similarly, the value of the overall exergy efficiency improves from 0.421 to 0.7099, indicating a significant improvement of about 69%. This can be related to the fact that a rise in the turbine inlet temperature reduces the irreversibilities of the ORC cycle, specifically the boiler and turbine components, thereby increasing the potential of exergy recovery.

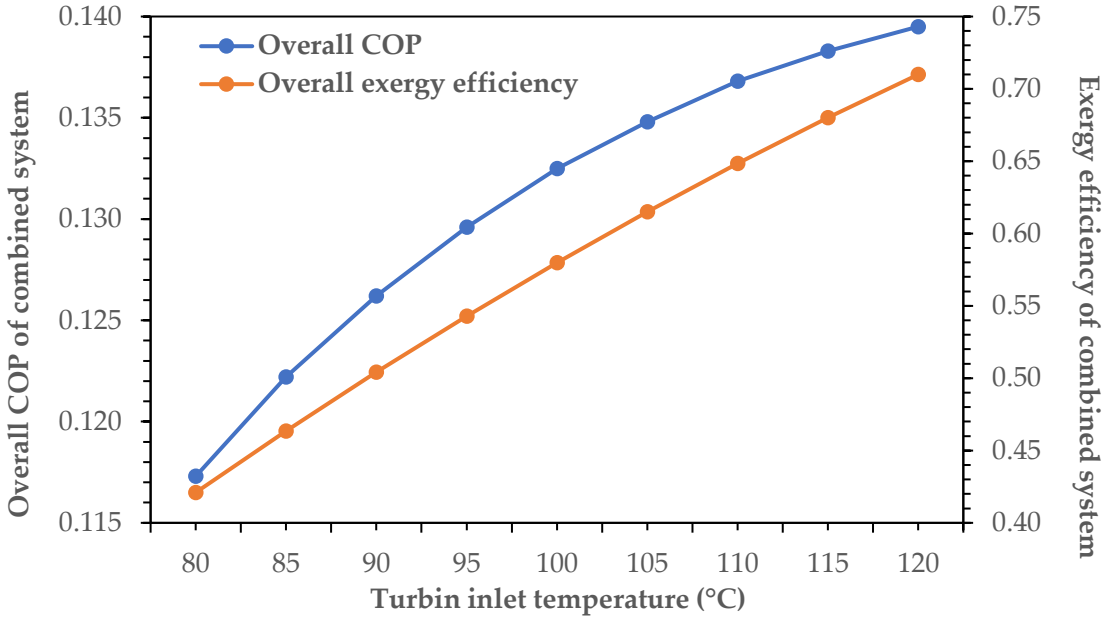


**Figure 9.** The variation of overall COP and exergy efficiency of ORC-VCC system with turbin inlet temperature (Fixed: ORC and VCC condenser temperatures of 40°C, VCC evaporator temperature of 5°C)

The variation of overall COP and exergy efficiency of ORC-VCC system with condenser temperature of ORC is shown in Figure 10. Overall COP decreases from 0.1432 to 50°C to 0.111 at 50°C, which shows a COP reduction of about 22% with a temperature increase in the ORC condenser. As a result of the increase in ORC condenser temperatures, the condensation pressures increase, which in turn reduces the net work output of the turbine as well as increases the rate of exergy destruction during the condensation process. The above-mentioned processes lead to a decrease in the power output to VCC's compressor, thereby reducing the overall COP. However, during this period, the overall exergy efficiency reduces from 0.6266 to 0.486, which shows a fall of about 22.4%. The increase in condensation temperatures increases heat-rejection irreversibilities. Moreover, it increases the temperature difference between the working fluid as well as the heat reservoir. As a consequence, both cycles experience a deterioration in their thermodynamic performance because higher temperatures in the ORC condenser have a direct effect on reducing ORC's output power, as well as increasing the rate of entropy generation.

The variation of overall COP and exergy efficiency of ORC-VCC system with condenser temperature of VCC is shown in Figure 11. With an increase in VCC condenser temperature from 35°C to 50°C, there is a

reduction in overall COP values from 0.1572 to 0.09946, showing a reduction of almost 37%. As condensation temperatures rise, so does the discharge pressure of the compressor, thereby increasing compression work. Because of this, as a result of increasing loads on the ORC turbine, thermodynamic coupling conditions deteriorate. Therefore, exergy efficiency values reduce from 0.6882 to 0.4353, showing a reduction of almost 37%. Higher condensation temperatures cause more irreversibilities in VCC condenser as a result of larger temperature differences and enhanced throttling effects downstream. Therefore, VCC system conditions become more thermodynamically challenging, thereby consuming more power from ORC turbine and hence deteriorating system performance.

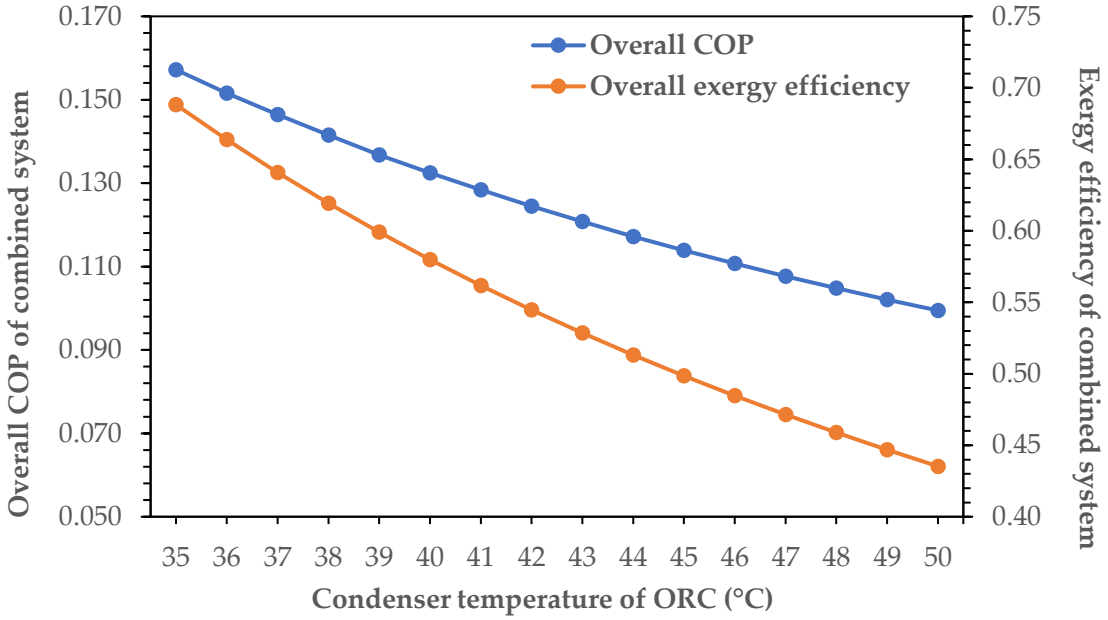


**Figure 10.** The variation of overall COP and exergy efficiency of ORC-VCC system with condenser temperature of ORC (Fixed: VCC condenser temperature of 40°C, VCC evaporator temperature of 5°C, turbine inlet temperature of 100°C)

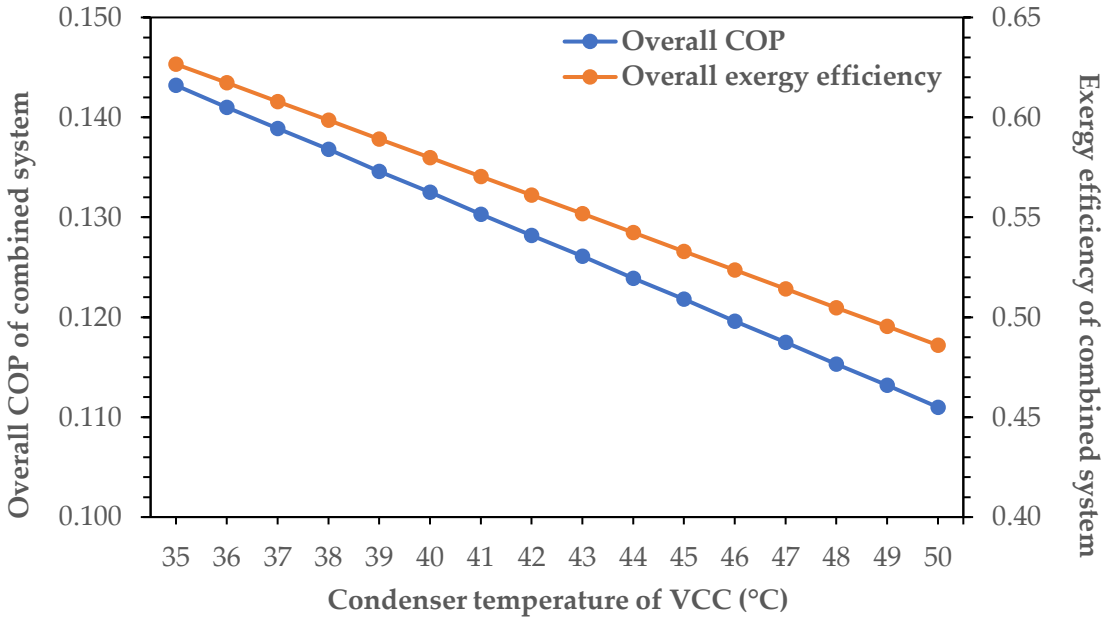


**Figure 11.** The variation of overall COP and exergy efficiency of ORC-VCC system with condenser temperature of VCC (Fixed: VCC condenser temperature of 40°C, VCC evaporator temperature of 5°C, turbine inlet temperature of 100°C)

The variation of overall COP and exergy efficiency of ORC-VCC system with evaporator temperature of VCC is shown in Figure 12. Overall COP of the combined system is reduced from 0.1761 at −10 °C to 0.1047 at 10 °C, which is a drop of approximately 40% with the rise in the evaporator temperature. This is rather puzzling, since the cooling demand, or the enthalpy difference across the evaporator, is a decreasing function of the evaporating temperature, whereas the work input from the Organic Rankine Cycle is more or less the same. Thus, the cooling capacity per unit compressor work input is reduced. Conversely, the total exergy efficiency is improved from 0.365 to 0.6998, which is a near doubling. Higher evaporator temperatures can mitigate the irreversibilities involved in the evaporation at low pressure, the entropy generation, and the thermodynamic quality of the heat absorption process. Thus, the system provides less cooling but at a higher exergy efficiency, which shows that the energetic and exergetic behaviors can be different depending on the entropy generation distribution in the VCC evaporator.

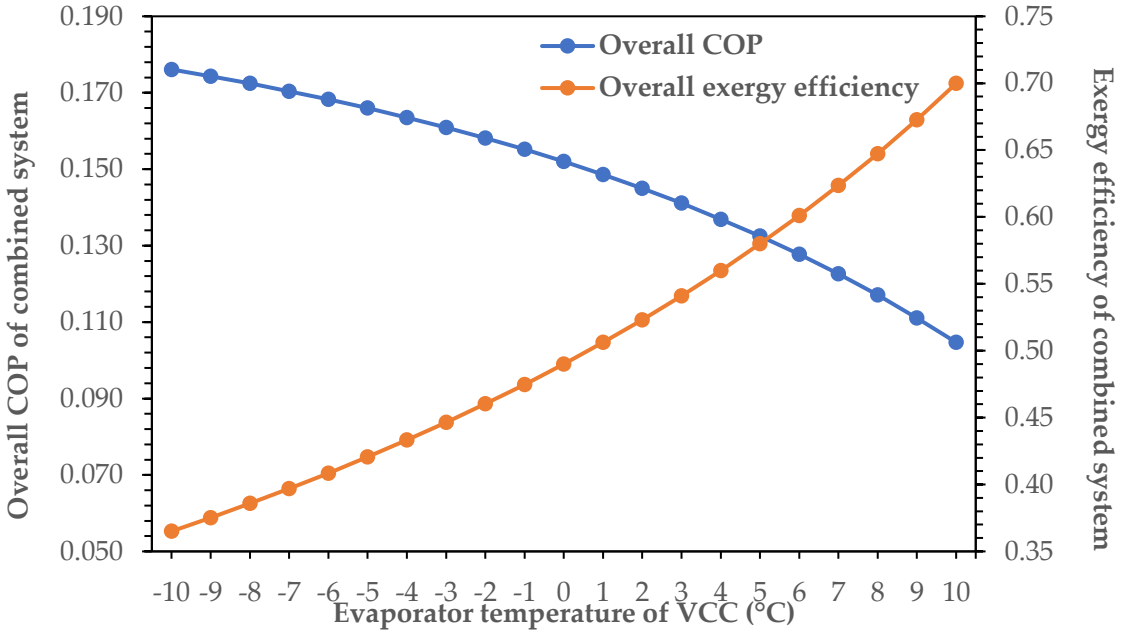


**Figure 12.** The variation of overall COP and exergy efficiency of ORC-VCC system with evaporator temperature of VCC (Fixed: ORC and VCC condenser temperatures of 40°C, turbine inlet temperature of 100°C)

On the basis of the comparative performance analysis of all the selected working fluid pairs, R1336mzz(Z) for the ORC and R1233zd(E) for the VCC are found to be the most preferable fluids for the given working conditions. A detailed analysis of the thermodynamic state points is, therefore, carried out for the combined ORC and VCC system with the mentioned preferable fluid pair. The thermodynamic properties such as temperature, pressure, specific enthalpy, and specific entropy of the combined system at various states are listed in Table 7 in a tabulated form to provide a quantitative understanding of the behavior of the system for the preferable pair of fluids. The fixed outlet temperatures are as follows: VCC evaporator outlet at 5 °C with saturated vapor state; VCC condenser outlet at 40 °C with saturated liquid state; ORC condenser outlet at 40 °C with saturated liquid state; and ORC evaporator outlet/turbine inlet at 100 °C with saturated vapor state. The isentropic efficiencies of the pump, turbine, and compressor are fixed at 0.80, 0.75, and 0.75, respectively. The efficiency of the internal heat exchanger (ε) is kept constant at 0.70 for all cases. The mass flow rate of the working fluid in the VCC system is obtained from an energy balance at the evaporator based on the fixed cooling capacity. The mass flow rate of the working fluid in the ORC system is obtained by imposing the coupling condition of equal power extracted by the compressor and that available at the turbine. The mass flow rates of the hot and cold streams in the IHX are obtained as a result of an energy balance in each of the respective cycles.

**Table 7.** Thermodynamic properties of each state of the combined system

| State | T (°C) | P (kPa) | h (kJ/kg) | s (kJ/kg/°C) | ṁ (kg/s) | x (-) |
|---|---|---|---|---|---|---|
| 1 | 5 | 59.41 | 408.4 | 1.75 | 0.05602 | 1 |
| 2 | 29.5 | 59.41 | 428.2 | 1.818 | 0.05602 | |
| 3 | 72.75 | 215.4 | 461.9 | 1.842 | 0.05602 | |
| 4 | 40 | 215.4 | 249.7 | 1.169 | 0.05602 | 0 |
| 5 | 24.22 | 215.4 | 229.9 | 1.105 | 0.05602 | |
| 6 | 5 | 59.41 | 229.9 | 1.108 | 0.05602 | |
| 7 | 40 | 128 | 249.6 | 1.169 | 0.09074 | 0 |
| 8 | 40.47 | 707.1 | 250.2 | 1.171 | 0.09074 | |
| 9 | 60.16 | 707.1 | 275.8 | 1.249 | 0.09074 | |
| 10 | 100 | 707.1 | 460.4 | 1.752 | 0.09074 | 1 |
| 11 | 68.6 | 128 | 439.6 | 1.772 | 0.09074 | |
| 12 | 41.28 | 128 | 414 | 1.694 | 0.09074 | |

## 4. Conclusion

In this study, a thermodynamics analysis of an integrated ORC-VCC with fixed operating conditions for sixteen different pairs of working fluids is carried out. It is shown by the results that the selection of working fluids significantly affects the performance indicators of the subsystems as well as the total system performance. The power of the ORC turbine varies between 1.795 kW and 1.962 kW, with an absolute difference of 0.167 kW or about 8.5%. Additionally, the thermal efficiency of the ORC is limited to a small range of 0.1008-0.1093, with a maximum relative improvement of 7.8%, while that of the exergy efficiency for the ORC is between 0.4347 and 0.4716, with an improvement of 8.5%. In the refrigeration application area, the COP of the VCC is enhanced from 4.95 to 5.303, registering a relative improvement of about 7.1%. The VCC exergy efficiency is seen to increase systematically from 0.2622 to 0.2809, registering a percentage improvement of about 7.1%. These observations indicate that the refrigeration system is increasingly responding to the fluid selection process with a moderate improvement of numerical values. Being the collective result of the two cycles, the COP of the total system increases from 0.4989 to 0.5799, indicating a relative improvement of 16.2%. Similarly, the total system exergy efficiency also increases from 0.1140 to 0.1325, indicating a relative improvement of 16.2%. This relative improvement in both instances suggests the collective effect that is achieved by improving the performance of both ORC and VCC. When comparing the results among all cases, the models FP-12 and FP-16 always obtain the maximum values of turbine power, COP of the total system, and system exergy efficiency, signifying that these models perform better. On the contrary, models FP-3, FP-7, FP-11, and FP-15 produce the lowest results for various indicators of performance.

Apart from the results in the fixed conditions, the numerical results of the parametric analysis can also validate the system performance. Raising the turbine inlet temperature from 80 °C to 120 °C can improve the COP from 0.1173 to 0.1395 (about 19%) and the exergy efficiency from 0.421 to 0.7099 (about 69%). Raising the condenser temperature of the ORC from 35 °C to 50 °C can decrease the COP from 0.1432 to 0.111 (about 22%) and the exergy efficiency from 0.6266 to 0.486 (about 22.4%). Raising the condenser temperature of the VCC from 35 °C to 50 °C can decrease the COP from 0.1572 to 0.09946 (about 37%) and the exergy efficiency from 0.6882 to 0.4353 (about 37%). Finally, raising the evaporator temperature of the VCC from −10 °C to 10 °C can decrease the COP from 0.1761 to 0.1047 (about 40%) but can improve the exergy efficiency from 0.365 to 0.6998 (about 92%). These numerical results can clearly demonstrate the system's sensitivity to the specified temperature factors, which can also indicate that the COP and exergy efficiency can have opposite variation tendencies depending on the dominant irreversibility.
These results make it clear that the integration of ORC and VCC is a solution with a positive effect on the environment because it has high efficiency in applications such as recovery of waste heat, use of low-temperature geothermal resources, and management of industrial process heat and data center cooling.

## Author Contributions

The author solely conducted the investigation, conceptualization, system design, data collection, analysis, and interpretation, and was fully responsible for writing and revising the manuscript.

## Conflict of Interest

The author of the article declares that he has no personal or financial conflict of interest with any institution, organization or person.

## References

[1] Almehmadi FA, Elattar HF, Fouda A, Alqaed S, Mustafa J, Alharthi MA, Refaey HA. Energy performance assessment of a novel solar poly-generation system using various ORC working fluids in residential buildings. Energies 2022;15:8286.
[2] Almehmadi FA, Elattar HF, Fouda A, Alqaed S, Alharthi MA, Refaey HA. Towards an efficient multi-generation system providing power, cooling, heating, and freshwater for residential buildings operated with solar-driven ORC. Applied Sciences 2022;12:11157.
[3] Kaczmarczyk TZ, Żywica G. Experimental study of the effect of load and rotational speed on the electrical power of a high-speed ORC microturbogenerator. Applied Thermal Engineering 2024;238:122012.
[4] Pan M, Zhao H, Liang D, Zhu Y, Liang Y, Bao G. A review of the cascade refrigeration system. Energies 2020;13:2254.
[5] Saeed MZ, Contiero L, Blust S, Allouche Y, Hafner A, Eikevik TM. Ultra-low-temperature refrigeration systems: A review and performance comparison of refrigerants and configurations. Energies 2023;16:7274.
[6] Tassou SA, Lewis JS, Ge YT, Hadawey A, Chaer I. A review of emerging technologies for food refrigeration applications. Applied Thermal Engineering 2010;30:263–276.
[7] Lecompte S, Huisseune H, Van Den Broek M, Vanslambrouck B, De Paepe M. Review of organic Rankine cycle (ORC) architectures for waste heat recovery. Renewable and Sustainable Energy Reviews 2015;47:448–461.
[8] Aphornratana S, Sriveerakul T. Analysis of a combined Rankine–vapour-compression refrigeration cycle. Energy Conversion and Management 2010;51:2557–2564.
[9] Wang H, Peterson R, Herron T. Design study of configurations on system COP for a combined ORC (organic Rankine cycle) and VCC (vapor compression cycle). Energy 2011;36:4809–4820.
[10] Toujeni N, Bouaziz N, Kairaouani L. Energetic investigation of a new combined ORC-VCC system for cogeneration. Energy Procedia 2017;139:670–675.
[11] Asim M, Leung MKH, Shan Z, Li Y, Leung DYC, Ni M. Thermodynamic and thermo-economic analysis of integrated organic Rankine cycle for waste heat recovery from vapor compression refrigeration cycle. Energy Procedia 2017;143:192–198.
[12] Aryanfar Y, Assad MEH, Khosravi A, Atiqure RSM, Sharma S, Alcaraz JLG, Alayi R. Energy, exergy and economic analysis of combined solar ORC-VCC power plant. International Journal of Low-Carbon Technologies 2022;17:196–205.
[13] Nasir MT, Kim KC. Working fluids selection and parametric optimization of an organic Rankine cycle coupled vapor compression cycle (ORC-VCC) for air conditioning using low grade heat. Energy and Buildings 2016;129:378–395.
[14] Karellas S, Braimakis K. Energy-exergy analysis and economic investigation of a cogeneration and trigeneration ORC-VCC hybrid system utilizing biomass fuel and solar power. Energy Conversion and Management 2016;107:103–113.
[15] Grauberger A, Young D, Bandhauer T. Off-design performance of an organic Rankine–vapor compression cooling cycle using R1234ze(E). Applied Energy 2022;321:119421.
[16] Grauberger A, Young D, Bandhauer T. Experimental validation of an organic Rankine–vapor compression cooling cycle using low GWP refrigerant R1234ze(E). Applied Energy 2022;307:118242.
[17] Sleiti AK, Al-Ammari WA, Al-Khawaja M. Experimental investigations on the performance of a thermo-mechanical refrigeration system utilizing ultra-low temperature waste heat sources. Alexandria Engineering Journal 2023;71:591–607.
[18] Asim M, Kashif F, Umer J, Alvi JZ, Imran M, Khan S, Zia AW, Leung MKH. Performance assessment and working fluid selection for novel integrated vapor compression cycle and organic Rankine cycle for ultra low grade waste heat recovery. Sustainability 2021;13:11592.

[19] Pektezel O, Acar HI. Energy and exergy analysis of combined organic Rankine cycle-single and dual evaporator vapor compression refrigeration cycle. Applied Sciences 2019;9(23):5028.
[20] Bademlioğlu A, Canbolat A, Yamankaradeniz N, Kaynaklı Ö. A parametric analysis of the performance of organic Rankine cycle with heat recovery exchanger and its statistical evaluation. Isı Bilimi ve Tekniği Dergisi 2019;39(2):121–135.
[21] Alshammari, S., Kadam, S. T., Yu, Z. Assessment of single rotor expander-compressor device in combined organic Rankine cycle (ORC) and vapor compression refrigeration cycle (VCR). Energy 2023;282:128763.
[22] Bu XB, Li HS, Wang LB. Performance analysis and working fluids selection of solar powered organic Rankine–vapor compression ice maker. Solar Energy 2013;95:271–278.
[23] González J, Llovell F, Garrido JM, Quinteros-Lama H. Selection of a suitable working fluid for a combined organic Rankine cycle coupled with compression refrigeration using molecular approaches. Fluid Phase Equilibria 2023;572:113847.
[24] Bounefour O, Ouadha A, Addad Y. An exergy analysis of various layouts of ORC–VCC systems for usage in waste heat recovery on board ships. Marine Systems & Ocean Technology 2020;15:26–44.
[25] Ngangué MN, Lekané NN, Njock JP, Sosso OT, Stouffs P. Working fluid selection for a high efficiency integrated power/cooling system combining an organic Rankine cycle and vapor compression–absorption cycles. Energy 2023;277:127709.
[26] Zhar R, Allouhi A, Ghodbane M, Jamil A, Lahrech K. Parametric analysis and multi-objective optimization of a combined organic Rankine cycle and vapor compression cycle. Sustainable Energy Technologies and Assessments 2021;47:101401.
[27] Xia XX, Liu ZP, Wang ZQ, Sun T, Zhang HL. Multi-layer performance optimization based on operation parameter–working fluid–heat source for the ORC–VCR system. Energy 2023;272:127103.
[28] Zheng N, Wei JJ, Zhao L. Analysis of a solar Rankine cycle powered refrigerator with zeotropic mixtures. Solar Energy 2018;162:57–66.
[29] Ashwni SAF, Tiwari D. Thermodynamic analysis of simple and modified organic Rankine cycle and vapor compression refrigeration systems. Environmental Progress & Sustainable Energy 2021;40:13577.
[30] Karellas S, Braimakis K. Energy–exergy analysis and economic investigation of a cogeneration and trigeneration ORC–VCC hybrid system utilizing biomass fuel and solar power. Energy Conversion and Management 2016;107:103–113.
[31] Saleh B. Energy and exergy analysis of an integrated organic Rankine cycle–vapor compression refrigeration system. Applied Thermal Engineering 2018;141:697–710.
[32] Javanshir N, Seyed Mahmoudi SM, Rosen MA. Thermodynamic and exergoeconomic analyses of a novel combined cycle comprised of vapor-compression refrigeration and organic Rankine cycles. Sustainability 2019;11:3374.
[33] Bao J, Zhang L, Song C, Zhang N, Zhang XP, He GH. Comparative study of combined organic Rankine cycle and vapor compression cycle for refrigeration: single fluid or dual fluid? Sustainable Energy Technologies and Assessments 2020;37:100595.